Quantum correlations in the two-photon decay of few-electron ions

Filippo Fratini,[1,2,*] Malte C. Tichy,[3] Thorsten Jahrsetz,[1,2] Andreas Buchleitner,[3] Stephan Fritzsche,[2,4] and Andrey Surzhykov[1,2]
[1]*Physikalisches Institut, Ruprecht-Karls-Universität Heidelberg, Philosophenweg 12, D-69120 Heidelberg, Germany*
[2]*GSI Helmholtzzentrum für Schwerionenforschung, D-64291 Darmstadt, Germany*
[3]*Physikalisches Institut, Albert-Ludwigs-Universität Freiburg, Hermann-Herder Strasse 3, D-79104 Freiburg, Germany*
[4]*FIAS Frankfurt Institute for Advanced Studies, D-60438 Frankfurt am Main, Germany*
(Received 24 November 2010; published 21 March 2011)

A theoretical study of the polarization entanglement of two photons emitted in the decay of metastable ionic states is performed within the framework of density-matrix theory and second-order perturbative approach. Particular attention is paid to relativistic and nondipole effects that become important for medium- and high-Z ions. To analyze these effects, the degree of entanglement is evaluated both in the dipole approximation and within rigorous relativistic theory. Detailed calculations are performed for the two-photon $2s_{1/2} \to 1s_{1/2}$ transition in hydrogenlike ions as well as for the $1s_{1/2}\,2s_{1/2}\,{}^1S_0 \to 1s^2_{1/2}\,{}^1S_0$, $1s_{1/2}\,2s_{1/2}\,{}^3S_1 \to 1s^2_{1/2}\,{}^1S_0$, and $1s_{1/2}\,2p_{1/2}\,{}^3P_0 \to 1s^2_{1/2}\,{}^1S_0$ transitions in heliumlike ions.

DOI: 10.1103/PhysRevA.83.032506 PACS number(s): 32.10.−f, 31.10.+z, 03.67.Bg, 03.65.Ud

I. INTRODUCTION

Over the decades, two-photon bound-bound transitions in atoms and ions have provided a unique testing ground for advanced atomic theories. Starting from the early work by Göppert-Mayer [1] and Breit and Teller [2], a large number of theoretical studies were carried out to estimate the total as well as the energy- and angle-differential (two-photon) decay rates [3–10]. When compared with experimental data [11–15], these studies revealed important information on relativistic, quantum electrodynamics, and many-body phenomena in atomic systems. Besides structure-related investigations, more recent interest focuses on the quantum correlations between the emitted photons, which can be used to probe fundamental aspects of modern quantum theory. In a series of studies, for example, photon-photon polarization correlations were employed to test the Bell inequality [16–18]. In particular, these investigations demonstrated that the polarization correlations cannot be explained by any local realistic theory that uses hidden variables. Hence, together with other Bell test experiments, two-photon studies proved that nature indeed exhibits quantum-mechanical nonlocality. These results contributed to the long-lasting historical debate of Einstein with Bohr and Schrödinger [19,20], who introduced the notion of entanglement for denoting nonproduct (pure) states.

In the past, both experimental [17] and theoretical [21,22] studies of γ-γ polarization correlation were mainly restricted to the $2s \to 1s$ decay of neutral hydrogen (or deuterium). Much less attention was paid to two-photon transitions in other atomic or ionic species. With the recent advances in heavy-ion accelerator and trap facilities as well as in x-ray detection techniques, concrete possibilities arise to study spin-correlation phenomena in the decay of heavy, few-electron ions. In the medium- and high-Z domain, however, a proper analysis of polarization quantum correlations requires detailed knowledge of relativistic effects and many-electron effects, as well as of those contributions that arise from the higher-order (nondipole) terms in the expansion of the electron-photon interaction.

In this paper we investigate quantum correlations between the polarization states of two photons emitted in the decay of few-electron ions. Most naturally, spin-correlation phenomena are described within the framework of density-matrix theory. However, before we present details from this theory, we first summarize the geometry under which the two-photon decay is considered in Sec. II. Then in Sec. III A the general expression for the spin-density matrix of the photon pair is derived in terms of the initial populations of the ionic substates as well as in terms of the (second-order) transition amplitudes. The evaluation of these amplitudes in relativistic, second-order perturbation theory is thereafter discussed for hydrogenlike and heliumlike ions. For the latter species, we make use of the independent-particle model, which is appropriate for the analysis of bound-state transitions in the high-Z domain [23,24]. Apart from rigorous relativistic results, we also present simplified expressions describing the photons' polarization state within the dipole approximation. These intuitive expressions, derived in Sec. III B, will enable us to understand the general behavior of polarization correlations. In order to provide a quantitative description for these correlations, we briefly recall in Sec. IV the definition of concurrence as the measure of entanglement. Fully relativistic calculations of the concurrence are then performed for the $2s_{1/2} \to 1s_{1/2}$ transition in hydrogenlike ions, as well as for the $1s_{1/2}\,2s_{1/2}\,{}^1S_0 \to 1s^2_{1/2}\,{}^1S_0$, $1s_{1/2}\,2s_{1/2}\,{}^3S_1 \to 1s^2_{1/2}\,{}^1S_0$, and $1s_{1/2}\,2p_{1/2}\,{}^3P_0 \to 1s^2_{1/2}\,{}^1S_0$ transitions in heliumlike ions. The results of these calculations are displayed in Sec. V and are compared to the predictions based on the dipole approximation. From this comparison we infer the twofold impact of relativity on polarization entanglement: Apart from (i) the loss of purity of the photon states, (ii) the relativistic contraction of the wave functions and the nondipole contributions to the electron-photon interaction generally lead to the reduction of concurrence—an effect that becomes prominent for heavy ions and high photon energies. A brief summary, together with some perspectives, is given in Sec. VI.

Atomic units are used throughout the paper, unless stated otherwise.

*fratini@physi.uni-heidelberg.de

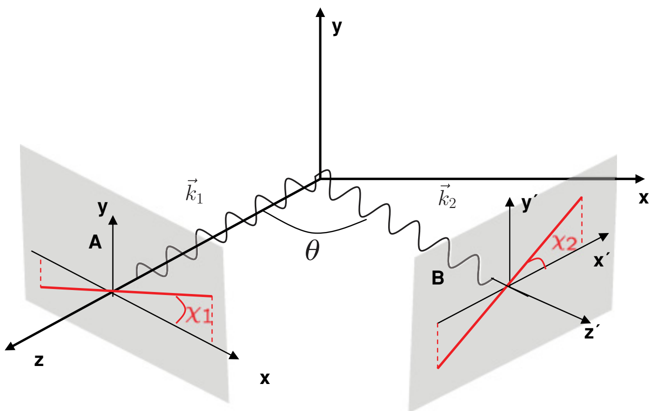

FIG. 1. (Color online) General decay geometry. The z axis is oriented in the direction of the photon with momentum $\vec{k}_1$, measured by the detector A. Together with the emission direction of the second photon, it defines the x-z reaction plane. The opening angle between both photons is denoted by θ, while the (linear) polarization angles of the photons, measured with respect to the x-z plane, are denoted by χ_1 and χ_2, respectively.

II. GEOMETRY OF THE SETUP AND THE PHOTON LABELING PROBLEM

In order to analyze γ-γ polarization correlations, we first introduce the geometry of the two-photon emission. Since, for the decay of unpolarized ions, there is no direction initially preferred for the overall system, we adopt the momentum of the first photon to coincide with the z axis, which is also taken to be the quantization axis. Together with the direction of the second photon, this axis defines the reaction plane (the x-z plane). A single opening angle θ is therefore required to characterize the emission of the photons with respect to each other (see Fig. 1).

Since the two photons are in a symmetrized state, it is *a priori* not possible to address them individually. However, we can safely assume that photons observed by the detectors have definite energies and momenta, i.e., they collapse onto energy and momentum eigenstates. Therefore a clear identity can be given to the photons [25]: the first (second) photon is the one detected by the detector A (B) (marked gray in Fig. 1) at a certain energy $\omega_{1(2)}$ and with momentum $\vec{k}_{1(2)}$. By distinguishing the photons in such a way, we can use their polarization states in order to investigate the associated entanglement properties. Indeed, such an analysis is possible since—in contrast to the energy and momentum spaces—the photon spin state can be directly measured in any basis.

III. THEORY

A. Density-matrix approach

Having defined the geometry of the two-photon decay, we shall next recall the theoretical background needed to investigate the polarization of the emitted radiation. Most naturally, polarization-correlation studies can be performed in terms of the system's density matrix. Since this approach was recently applied to describe two-photon transitions in hydrogenlike ions [21,22], here we restrict ourselves to a short compilation of the basic formulas relevant to our further analysis.

The initial state of the overall system in our two-photon decay problem is given by the photon vacuum $|\text{vac}\rangle \equiv |0,0\rangle_{i,\gamma}$ and by the excited ion (or atom) in states $|\alpha_i, J_i, M_i\rangle$ with well-defined total angular momentum J_i and associated projection M_i onto the z axis. Moreover, α_i is a collective label for all additional quantum numbers required for a unique specification of the state. In particular, it characterizes electronic configurations that give rise to the state and hence provides its parity P_i.

The magnetic sublevel population of the ion in initial states is described as a statistical mixture by the density operator

$$\hat{\rho}_{i,\text{ion}} = \sum_{M_i} C_{M_i} \, |\alpha_i, J_i, M_i\rangle \, \langle \alpha_i, J_i, M_i| \, , \tag{1}$$

where C_{M_i} denotes the population of the magnetic substate $|\alpha_i, J_i, M_i\rangle$. Since in most (two-photon) experiments, the initially prepared excited ionic states are unpolarized, we fix the parameters as $C_{M_i} = 1/(2J_i + 1)$. Such a realistic choice for the initial-state population has important consequences for the (spin) entanglement of emitted photon pairs. As we will see later, by introducing the incoherent mixture of initial magnetic substates [Eq. (1)], the two-photon state's coherences are jeopardized as well and hence a loss of quantum correlations is induced.

The density (statistical) operators of the initial and the final states of the overall system are connected by the standard relation [26–28]

$$\hat{\rho}_f = \hat{U} \, \hat{\rho}_{i,\text{ion}} \otimes \hat{\rho}_{i,\gamma} \, \hat{U}^\dagger, \tag{2}$$

where $\hat{U}$ is the evolution operator, which accounts for the interaction of the ion with the radiation field. The final-state operator [Eq. (2)] describes both the deexcited ion in some state $|\alpha_f, J_f, M_f\rangle$ and the two emitted photons with momenta $\vec{k}_{1,2}$ and helicities $\lambda_{1,2}$. Owing to the transverse character of the electromagnetic radiation, these helicities, or projections of the photon momenta on their own directions of propagation, can take only two values, $\lambda_{1,2} = \pm 1$.

Instead of using the final-state density operator $\hat{\rho}_f$, it is often more convenient to work with its matrix representation, briefly referred to as the final-state density matrix. In the representation of the individual angular momenta this matrix reads

$$\begin{aligned}
&\langle f; \vec{k}_1\lambda_1, \vec{k}_2\lambda_2 | \hat{\rho}_f | f'; \vec{k}_1\lambda_1', \vec{k}_2\lambda_2' \rangle \\
&\quad \equiv \langle \alpha_f J_f M_f; \vec{k}_1\lambda_1, \vec{k}_2\lambda_2 | \hat{\rho}_f | \alpha_f J_f M_f'; \, \vec{k}_1\lambda_1', \vec{k}_2\lambda_2' \rangle \\
&\quad = \frac{1}{2J_i + 1} \sum_{M_i} C_i \mathcal{M}_{fi}^{\vec{k}_1\vec{k}_2}(\lambda_1, \lambda_2) \mathcal{M}_{fi}^{\vec{k}_1\vec{k}_2 \, *}(\lambda_1', \lambda_2'),
\end{aligned} \tag{3}$$

where we employed Eq. (1) to evaluate elements of the ionic initial-state matrix $\langle \alpha_i J_i M_i | \hat{\rho}_{i,\text{ion}} | \alpha_i J_i M_i' \rangle$ and introduced formal notation for the transition amplitude:

$$\mathcal{M}_{fi}^{\vec{k}_1\vec{k}_2}(\lambda_1, \lambda_2) = \langle \alpha_f J_f M_f; \vec{k}_1\lambda_1, \vec{k}_2\lambda_2 | \hat{U} | \alpha_i J_i M_i; 0,0 \rangle. \tag{4}$$

As seen from this expression, $\mathcal{M}_{fi}^{\vec{k}_1\vec{k}_2}(\lambda_1,\lambda_2)$ describes a transition between two bound ionic states accompanied by the simultaneous emission of two photons.

The final-state matrix [Eq. (3)] still contains the complete information about the system and can be used to derive the properties of the photons or the residual ion. Assuming that the final magnetic substate of the ion remains unobserved in an experiment, we can derive the reduced density matrix $\hat{\rho}_\gamma$, which describes only the polarization state of the two photons, measured at a certain opening angle θ, with certain energies ω_1 and ω_2:

$$\begin{aligned}
&\langle \vec{k}_1,\lambda_1,\vec{k}_2,\lambda_2|\hat{\rho}_{f,\gamma}\,|\vec{k}_1,\lambda_1',\vec{k}_2,\lambda_2'\rangle \\
&\quad\equiv \sum_{M_f} \langle f;\vec{k}_1,\lambda_1,\vec{k}_2,\lambda_2|\hat{\rho}_f\,|f;\vec{k}_1,\lambda_1',\vec{k}_2,\lambda_2'\rangle \\
&\quad= \frac{\mathcal{N}}{2J_i+1}\sum_{M_i,M_f} C_{M_i}\mathcal{M}_{fi}^{\vec{k}_1\vec{k}_2}(\lambda_1,\lambda_2)\mathcal{M}_{fi}^{\vec{k}_1\vec{k}_2\,*}(\lambda_1',\lambda_2'), \qquad (5)
\end{aligned}$$

where we introduced the factor $\mathcal{N}$ to ensure the proper normalization of the matrix $\mathrm{Tr}(\hat{\rho}_\gamma)=1$. In what follows we will use this (reduced) matrix to analyze the polarization entanglement of the photons' pair. Before starting such an analysis, we shall briefly discuss the computation of the second-order amplitude [Eq. (4)]. Most naturally such an amplitude can be evaluated within the framework of second-order perturbation theory [6,26,27]:

$$\begin{aligned}
\mathcal{M}_{fi}^{\vec{k}_1\vec{k}_2}(\lambda_1,\lambda_2) = \sum\!\!\!\!\!\!\int_\nu \Bigg(&\frac{\langle f|\,\hat{\mathcal{R}}(\vec{k}_1,\lambda_1)|\nu\rangle\langle\nu|\hat{\mathcal{R}}(\vec{k}_2,\lambda_2)\,|i\rangle}{E_\nu - E_i + \omega_2} \\
&+ \frac{\langle f|\hat{\mathcal{R}}(\vec{k}_2,\lambda_2)\,|\nu\rangle\,\langle\nu|\,\hat{\mathcal{R}}(\vec{k}_1,\lambda_1)\,|i\rangle}{E_\nu - E_i + \omega_1}\Bigg). \qquad (6)
\end{aligned}$$

Here $|i\rangle = |\alpha_i,J_i,M_i\rangle$, $|\nu\rangle = |\alpha_\nu,J_\nu,M_\nu\rangle$, and $|f\rangle = |\alpha_f,J_f,M_f\rangle$ denote the solutions of Dirac's equation for the initial, intermediate, and final ionic states, respectively, while E_i, E_ν, and E_f are the corresponding energies. Because of energy conservation, E_i and E_f are related to the energies $\omega_{1,2}$ of the emitted photons by

$$E_i - E_f = \omega_1 + \omega_2. \qquad (7)$$

From this relation it is convenient to define the energy sharing parameter $\eta = \omega_1/(E_i - E_f)$, i.e., the fraction of energy that is carried away by the first photon.

In Eq. (6) $\hat{\mathcal{R}}(\vec{k},\lambda)$ is the transition operator that describes the relativistic interaction of the electrons with the electromagnetic radiation. In the velocity (Coulomb) gauge, this operator can be written as a sum of one-particle operators,

$$\hat{\mathcal{R}}^\dagger(\vec{k},\lambda) = \sum_m \vec{\alpha}_m \vec{\mathcal{A}}_{\lambda,m} = \sum_m \vec{\alpha}_m \vec{u}_\lambda e^{i\vec{k}\cdot\vec{r}_m}, \qquad (8)$$

where $\vec{\alpha}_m$ denotes the vector of the Dirac matrices for the mth particle, $\vec{\mathcal{A}}_{\lambda,m}$ is the vector potential of the photon field, and $\vec{u}_\lambda$ is the unit polarization vector. For practical computations, it is convenient to decompose the vector potential $\vec{\mathcal{A}}_{\lambda,m}$ into spherical tensors (i.e., into its electric and magnetic multipole components). For the emission of the photon in the direction $\hat{k} = (\theta,\phi)$ with respect to the quantization z axis, such a decomposition reads

$$\begin{aligned}
\vec{\mathcal{A}}_{\lambda,m} = \sqrt{2\pi}\sum_{L_\gamma=1}^{\infty}\sum_{M_\gamma=-L_\gamma}^{L_\gamma}\sum_{p=0,1} i^{L_\gamma}[L_\gamma]^{1/2}(i\lambda)^p \\
\times\, \hat{a}^p_{L_\gamma M_\gamma}(k) D^{L_\gamma}_{M_\gamma\lambda}(\hat{k}), \qquad (9)
\end{aligned}$$

where $[L_\gamma] = 2L_\gamma + 1$, $k = |\vec{k}|$, $D^{L_\gamma}_{M_\gamma\lambda}$ is the Wigner rotation matrix of rank L_γ, and the $\hat{a}^{p=0,1}_{L_\gamma M_\gamma}(k)$ refer to magnetic ($p=0$) and electric ($p=1$) multipoles, respectively.

The great advantage of the multipole expansion [Eq. (9)], when compared to the plane-wave formulation on the right-hand side of Eq. (8), is that it provides a radial-angular representation of the photon wave function. Together with similar representations of the atomic wave functions it allows for significant simplification of the transition amplitude $\mathcal{M}_{fi}^{\vec{k}_1\vec{k}_2}(\lambda_1,\lambda_2)$ (see Ref. [9] for further details). Moreover, Eq. (9) gives a very useful tool for studying multipole effects in the electron-photon interaction. If, for example, the summation in Eq. (9) is restricted to the term with $L_\gamma = 1$ and $p = 1$, one obtains the electric dipole ($E1$) contribution, while the component with $L_\gamma = 1$ and $p = 0$ provides the magnetic dipole ($M1$) contribution, and so on.

As seen from Eq. (6), the evaluation of second-order transition amplitudes requires the summation over the complete spectrum of the ion. Within the relativistic framework, such a computation is not a simple task since it includes a summation over the discrete part of the Dirac spectrum as well as an integration over the positive- and negative-energy continua. A number of methods have been developed in the past decades to compute Eq. (6) consistently. Apart from a direct summation over just a few intermediate states that are close in energy to the states involved in the decay, the discrete-basis-set approach is widely employed nowadays in (relativistic as well as nonrelativistic) second-order calculations. Within this approach, a finite set of discrete pseudostates is constructed from some basis functions and utilized to compute the transition amplitude $\mathcal{M}_{fi}$ [8,29]. In the present work we use an alternative—the Green's-function approach—which helps to avoid the direct summation over the (virtual) intermediate states $|\nu\rangle = |\alpha_\nu,J_\nu,M_\nu\rangle$. In the framework of this alternative approach, moreover, we employ the Sturmian representation [30] of the radial components of the Green's function, which allows the analytical evaluation of the transition amplitude [Eq. (6)] as well as the entanglement measures.

In contrast to hydrogenlike ions, the relativistic second-order calculations for few-electron systems are more intricate since one has to take into account electron-electron interaction effects. In the high-Z domain, however, the radiative transitions in few-electron ions can be reasonably well understood within the independent-particle model. This model, which takes the Pauli principle into account, is especially justified for heavy species since the interelectronic effects scale with $1/Z$ and hence are much weaker than the electron-nucleus interaction. The great advantage of the independent-particle model is that it allows the decomposition of the many-body, second-order transition amplitudes in terms of their one-electron analogs (see Ref. [24] for further details). In Sec. V B we will apply this approach for the computation of the spin entanglement between photons emitted in the decay of heavy heliumlike ions.

B. Dipole approximation

1. $S \to S$ transitions

The reduced density matrix [Eq. (5)] contains complete information about the spin states of the photon pairs emitted in the decay of atoms or ions. Together with the transition amplitude [Eq. (6)], it is suitable to explore two-photon transitions also in the high-Z domain, where relativistic and nondipole effects are significant. However, before we perform such a fully relativistic analysis, let us restrict ourselves first to the non-relativistic dipole theory and derive approximate expressions for the description of the two-photon polarization states. As we will see later, this will provide intuitive insight into the entanglement properties of the photon pairs. Moreover, by comparing predictions of such a simplified dipole approach with the results of the fully relativistic theory, we will be able to identify the relativistic and multipole effects in the two-photon transitions.

By making use of the nonrelativistic dipole approximation for the electron-photon interaction and by restricting the intermediate-state summation to states $|\nu\rangle = |\alpha_\nu, J_\nu, M_\nu\rangle$ with definite momentum J_ν and parity P_ν, defined by dipole selection rules, it is possible to express the two-photon density matrix [Eq. (5)] in the form [22]

$$\begin{aligned} &\langle \vec{k}_1,\lambda_1,\vec{k}_2\lambda_2|\hat{\rho}_\gamma\, |\vec{k}_1,\lambda_1',\vec{k}_2,\lambda_2'\rangle \\ &\approx C\,\lambda_1\lambda_2\lambda_1'\lambda_2' \sum_{L,\mu_1\mu_2} D^L_{\mu_1\mu_2}(\hat{x}'\hat{y}'\hat{z}' \to \hat{x}\hat{y}\hat{z}) \\ &\quad\times \langle 1,\lambda_1,1,-\lambda_1'|L,\mu_1\rangle\langle 1,-\lambda_2,1,\lambda_2'|L,\mu_2\rangle \\ &\quad\times\left(\begin{Bmatrix} J_\nu & J_f & 1 \\ J_i & J_\nu & 1 \\ 1 & 1 & L\end{Bmatrix} + \begin{Bmatrix} 1 & 1 & L \\ J_\nu & J_\nu & J_i\end{Bmatrix}\begin{Bmatrix} 1 & 1 & L \\ J_\nu & J_\nu & J_f\end{Bmatrix}\right), \end{aligned} \tag{10}$$

where we employ the standard notation for the Wigner $6j$ and $9j$ symbols [28] and C is a normalization constant that absorbs the radial parts of the (dipole) transition amplitudes $\mathcal{M}_{fi}$. The final-state density matrix [Eq. (10)] therefore depends only on the symmetry of the initial and final ionic states as well as on the photons' helicities.

As mentioned above, Eq. (10) can be applied to the analysis of only those transitions that proceed—within the nonrelativistic picture—via intermediate (virtual) states $|\alpha_\nu, J_\nu, M_\nu\rangle$ having one particular set of values for the total angular momentum J_ν and parity P_ν. This is the case of the $1s_{1/2}\,2s_{1/2}\,{}^1S_0 \to 1s^2_{1/2}\,{}^1S_0$ transition in heliumlike ions, for which the intermediate-state summation in the amplitude [Eq. (6)] is restricted to the $n_\nu\,{}^1P_1$ levels only if one treats the electron-photon interaction in the dipole approximation. Our approach is also justified for the $2s_{1/2} \to 1s_{1/2}$ decay in hydrogenlike ions since the intermediate states $n_\nu p_{1/2}$ and $n_\nu p_{3/2}$ are degenerate in the nonrelativistic limit. In the following analysis, therefore, we shall restrict the discussion of the nonrelativistic dipole approximation [Eq. (10)] to these two transitions.

By inspecting Eq. (10) for the cases of the (nonrelativistic) $2s_{1/2} \to 1s_{1/2}$ and $1s_{1/2}\,2s_{1/2}\,{}^1S_0 \to 1s^2_{1/2}\,{}^1S_0$ transitions, it can be proven that the density matrix $\hat{\rho}_\gamma$ fulfills the relation $\mathrm{Tr}(\hat{\rho}_\gamma^2) = [\mathrm{Tr}(\hat{\rho}_\gamma)]^2 = 1$ and hence represents a pure quantum-mechanical spin state of the emitted photons. This pure state can be described by the state vector

$$\begin{aligned} |\Psi\rangle = -\frac{1}{2\sqrt{1+\cos^2\theta}}&[(\cos\theta - 1)(|{+}{+}\rangle + |{-}{-}\rangle) \\ &+ (\cos\theta + 1)(|{+}{-}\rangle + |{-}{+}\rangle)], \end{aligned} \tag{11}$$

as directly derived from Eq. (10). In this expression the prefactor arises due to the normalization condition $\langle\Psi|\Psi\rangle = 1$ and, for the sake of brevity, we use the notation $|\pm\rangle \equiv |\lambda = \pm 1\rangle$. Here and henceforth, whenever a state vector describing both photons appears, the first (second) index is to be attributed to the first (second) photon, the photons being identified and detected according to Sec. II. For the particular case of back-to-back photon emission ($\theta = \pi$), the vector [Eq. (11)] further simplifies to a Bell state:

$$|\Psi\rangle = \frac{1}{\sqrt{2}}(|{+}{+}\rangle + |{-}{-}\rangle)\,. \tag{12}$$

As seen from this expression, for the opening angle $\theta = \pi$, photons can only be detected having the same helicity. In the past, such a quantum correlation between the photons emitted in the $2s_{1/2} \to 1s_{1/2}$ decay of atomic deuterium has been employed for verifying a violation of Bell's inequality [18].

Instead of the helicity basis $|\lambda = \pm 1\rangle$, it is often more convenient to analyze the polarization correlations of two photons in terms of their linear polarization unit vectors. These vectors are defined in the plane perpendicular to the photon propagation axis and can be obtained by the standard transformations [31]:

$$\begin{aligned} |x\rangle &= \frac{1}{\sqrt{2}}(|+\rangle + |-\rangle), \\ |y\rangle &= \frac{i}{\sqrt{2}}(-|+\rangle + |-\rangle). \end{aligned} \tag{13}$$

They can be used to rewrite the state vector [Eq. (11)] in the xy representation as

$$|\Psi\rangle = -\frac{1}{\sqrt{1+\cos^2\theta}}[|yy\rangle + \cos\theta\,|xx\rangle]. \tag{14}$$

Since we just change the basis, the opening angle $\theta = \pi$ again corresponds to a Bell, i.e., maximally entangled, state. In contrast, in this representation [Eq. (14)] we immediately see that perpendicular emission under $\theta = \pi/2$ results in a product (nonentangled, or separable) photon spin state.

The quantitative analysis of entanglement for the emitted photon pair will be performed in the following sections based on our general expression [Eq. (10)] as well as on the dipole approximation [Eqs. (12)–(14)]. Before we start with such an analysis let us discuss some basic properties of the spin state [Eq. (14)]. We recall the typical experimental scenario in which both photons are detected by polarimeters whose transmission axes are characterized by the angles χ_1 and χ_2 with respect to the reaction (x-z) plane (see Fig. 1). Equation (14) predicts that after the first photon has been detected by the detector A (the first detector) with some defined (linear) polarization angle χ_1, the second photon collapses onto the vector:

$$|\Psi\rangle \to N(\sin\chi_1\,|y\rangle + \cos\theta\cos\chi_1\,|x\rangle), \qquad (15)$$

with N some normalization factor. It follows from Eq. (15) that the second photon is then found in a linearly polarized state. The direction of this linear polarization, characterized by the angle $\tilde{\chi}_2$, depends on the opening angle θ and on the polarization angle χ_1 of the first photon:

$$\tan\tilde{\chi}_2 = \frac{1}{\cos\theta}\tan\chi_1. \qquad (16)$$

As we will show later, such a definite (except for the opening angle $\theta = \pi/2$) correspondence between the linear polarizations does not generally imply maximal entanglement of the photon pairs. To understand this issue and to quantify the degree of entanglement we shall introduce the concurrence measure in Sec. IV.

2. $P \to S$ transitions

In contrast to the $S \to S$ transitions from above, the nonrelativistic dipole approximation [Eqs. (10)–(14)] cannot be applied to the analysis of the $1s_{1/2}\,2p_{1/2}\,{}^3P_0 \to 1s_{1/2}^2\,{}^1S_0$ decay of heliumlike ions. The principal reason for this failure is that the leading (electric-magnetic dipole) $E1M1$-$M1E1$ $1s_{1/2}\,2p_{1/2}\,{}^3P_0 \to 1s_{1/2}^2\,{}^1S_0$ transition may proceed via intermediate $1s_{1/2}\,n_\nu s_{1/2}\,{}^3S_1$ or $1s_{1/2}\,n_\nu p\,{}^3P_1$ states, thus giving rise to a double-slit picture. By taking into account such a Young-type interference and by restricting ourselves to the dipole ($E1M1$-$M1E1$) terms in the electron-photon interaction, we again find the photon pair in a pure state:

$$|\Psi\rangle = C\bigg(-\Sigma(\eta)\sin^2\frac{\theta}{2}\,|{+}{+}\rangle + \Delta(\eta)\cos^2\frac{\theta}{2}\,|{-}{+}\rangle - \Delta(\eta)\cos^2\frac{\theta}{2}\,|{+}{-}\rangle + \Sigma(\eta)\sin^2\frac{\theta}{2}\,|{-}{-}\rangle\bigg). \qquad (17)$$

Here C is the normalization constant and the energy-dependent functions $\Sigma(\eta) = S_{E1M1}(\omega_1) + S_{E1M1}(\omega_2) + S_{M1E1}(\omega_1) + S_{M1E1}(\omega_2)$ and $\Delta(\eta) = S_{E1M1}(\omega_1) - S_{E1M1}(\omega_2) - S_{M1E1}(\omega_1) + S_{M1E1}(\omega_2)$ are given in terms of the multipole, second-order reduced transition amplitudes $S_{L_1p_1,L_2p_2}(\omega)$ (see Ref. [24] for further details).

As seen from Eq. (17), the spin state of the photons emitted in the $1s_{1/2}\,2p_{1/2}\,{}^3P_0 \to 1s_{1/2}^2\,{}^1S_0$ transition depends on the energy sharing η. No simple analytical expression for this dependence can be derived in general, owing to the complicated structure of the functions $\Delta(\eta)$ and $\Sigma(\eta)$. However, if both photons carry away the same fraction of energy $\omega_1 = \omega_2$, the function $\Delta(\eta = 0.5)$ vanishes and the vector [Eq. (17)] represents a maximally entangled (Bell) state:

$$|\Psi\rangle = \frac{1}{\sqrt{2}}(-|{+}{+}\rangle + |{-}{-}\rangle) = -\frac{i}{\sqrt{2}}(|xy\rangle + |yx\rangle). \qquad (18)$$

By comparing this expression with Eq. (14), one can see that polarization properties of $P_0 \to S_0$ and $S_0 \to S_0$ (as well as nonrelativistic $s_{1/2} \to s_{1/2}$) transitions are rather different: While the photons emitted in the $S \to S$ transitions can be detected having parallel linear polarization vectors, the $P \to S$ decay should result in emission of the photon pair with orthogonal linear polarizations. Moreover, no angular dependence arises in the state vector [Eq. (18)], implying maximal entanglement between the photons' spins, irrespective of the particular decay geometry.

IV. ENTANGLEMENT OF THE TWO-PHOTON STATE

We are ready now to discuss the concept of entanglement for the emitted photon pairs and to introduce a proper measure for it. Let us first return to the full two-photon state, which accounts not only for the spin, but also for the spatial degrees of freedom. Within the nonrelativistic dipole approximation [Eq. (14)], such a state before its detection reads

$$|\Phi\rangle = N\int d\omega_1 d\omega_2 \delta(\omega_1+\omega_2-\Delta_\omega) f(\omega_1)|\omega_1\omega_2\rangle \times \int d\theta_1 d\theta_2 |\theta_1\theta_2\rangle[|yy\rangle + \cos(\theta_1-\theta_2)|xx\rangle] + (1 \leftrightarrow 2), \qquad (19)$$

where $(1 \leftrightarrow 2)$ denotes the previous terms but with all particles' labels exchanged and the state is normalized by virtue of the constant N. Moreover, $f(\omega_{1,2})$ is the energy probability density function of the decay, $\Delta_\omega = E_i - E_f$ is the transition energy, and $\theta_{1,2}$ are the angles that address the positions of the first and second photons in the reaction plane, respectively. Due to the integral over angles and energies, the above state cannot be written as a product state for the energies, the emission angles, or the polarization. It can hence be seen as highly entangled, in general.

In order to rigorously discuss entanglement, due to the identity of particles, a degree of freedom for discrimination is needed. The energy of the photons and their opening angles are an appropriate choice since one naturally projects onto energy and momentum eigenstates in the experiment. In the coincidence experiment displayed in Fig. 1, the two-photon state collapses onto a state with definite momenta, while the polarization can be measured in any basis. If the energies of the photons are equal and the emission directions are exactly the same, we are unable to identify two separate particles between which entanglement may be defined. As long as this is not the case, we identify the particle projected on the two energies and angles as the two distinct entities to which we can safely assign an entanglement measure [25]. Hence, even though we start with a rather complex state of identical particles in which no physical subsystem structure is apparent, we can effectively deal with the two-qubit system of polarized photons projected on energy and momentum states.

Having clarified the concept of the two-photon entanglement, we shall now introduce its quantitative measure. For a photon pair, which can be seen as a two-qubit system, it is convenient to describe the degree of entanglement by means of Wootter's concurrence $\mathcal{C}$ [32]. For an arbitrary two-qubit system described by the density operator $\hat{\rho}$ the concurrence is defined as

$$\mathcal{C} = \max(0, \sqrt{e_1} - \sqrt{e_2} - \sqrt{e_3} - \sqrt{e_4}), \qquad (20)$$

where $\sqrt{e_i}$ are the square roots of the eigenvalues of the operator $\hat{\rho}(\hat{\sigma}_2^{(1)} \otimes \hat{\sigma}_2^{(2)})\hat{\rho}^*(\hat{\sigma}_2^{(1)} \otimes \hat{\sigma}_2^{(2)})$ in descending order, $\hat{\rho}^*$ is the complex conjugate of $\hat{\rho}$, and $\hat{\sigma}_2^{(1,2)} = \hat{\sigma}_y^{(1,2)}$ are the Pauli matrices acting on the first and the second qubit, respectively. Before we discuss further the properties of the concurrence $\mathcal{C}$, let us first recall that it quantifies correlations that can be fully attributed to the entanglement. Biparticle states with vanishing concurrence can still exhibit correlations that are not, however, of quantum nature.

The definition in Eq. (20) can be simplified further if applied to a pure quantum-mechanical state described by a ket vector

$$|\beta\rangle = C_{aa}\,|aa\rangle + C_{ab}\,|ab\rangle + C_{ba}\,|ba\rangle + C_{bb}\,|bb\rangle\,, \quad (21)$$

where a and b are arbitrary two-dimensional basis states and C_{ij} are complex numbers. For this state the concurrence reads

$$\mathcal{C} = 2|C_{aa}C_{bb} - C_{ab}C_{ba}|. \quad (22)$$

By using this expression and Eq. (14), we immediately obtain the analytical expression

$$\mathcal{C}(\theta) = 2\frac{|\cos\theta|}{1+\cos^2\theta} \quad (23)$$

for the spin entanglement of the photons emitted in the $2s_{1/2} \to 1s_{1/2}$ and $1s_{1/2}\,2s_{1/2}\,{}^1S_0 \to 1s^2_{1/2}\,{}^1S_0$ transitions. We recall that Eq. (23) is obtained within the nonrelativistic dipole approximation and should be questioned in the high-Z domain, where higher-order and relativistic effects can play a significant role. To explore the influence of these effects on the photon spin entanglement, in Sec. V we will compare the predictions obtained from Eq. (23) with the rigorous relativistic calculations based on Eqs. (5), (6), and (20).

V. RESULTS AND DISCUSSION

A. Hydrogenlike ions

1. Polarization entanglement

After discussing the theoretical background of two-photon polarization studies, we are now prepared to analyze the influence of the relativistic and higher-multipole effects on quantum correlations between the emitted particles. We start our analysis with the $2s_{1/2} \to 1s_{1/2}$ decay of hydrogenlike ions, which is well established both in theory and in experiment. As shown above, the polarization properties of this transition can be described—within the nonrelativistic dipole approximation—by the state vector [Eq. (14)] and hence by the degree of entanglement [Eq. (23)]. The theoretical predictions obtained within such a nonrelativistic approach are displayed in Fig. 2 for the decay of neutral hydrogen as well as hydrogenlike xenon Xe^{53+} and uranium U^{91+} ions and are compared with the results of the rigorous relativistic treatment. In the relativistic treatment, one deals with the relativistic Dirac wave functions and includes the full interaction between the electron and the radiation field in the amplitude [Eq. (6)]. Relativistic as well as nonrelativistic dipole calculations of the concurrence [Eqs. (20)–(22)] are performed at two relative photon energies $\eta = 1/16$ (upper panel) and $\eta = 1/2$ (lower panel). As seen from the figure, in the case of equal energy sharing ($\eta = 1/2$), both approaches

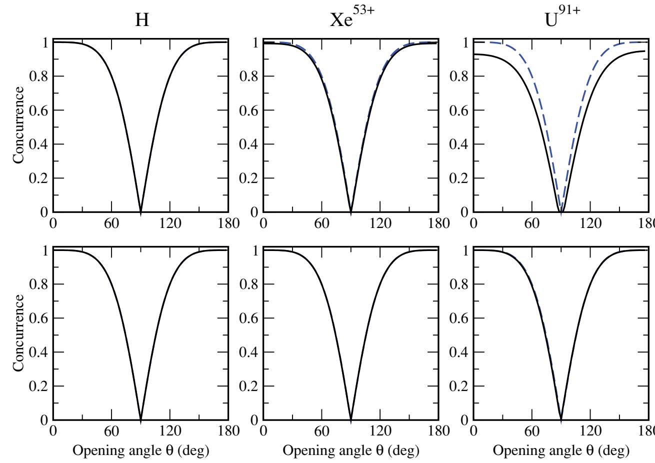

FIG. 2. (Color online) Concurrence of two photons emitted in the $2s_{1/2} \to 1s_{1/2}$ decay of neutral hydrogen and hydrogenlike xenon and uranium ions. The results of the nonrelativistic dipole approximation (dashed line) and the rigorous relativistic theory (solid line) are shown for two relative photon energies $\eta = 1/16$ (upper panel) and $\eta = 1/2$ (lower panel).

yield almost identical results along the entire isoelectronic sequence. Our calculations show that, while being maximal for the parallel ($\theta = 0$) and back-to-back ($\theta = \pi$) photon emission, the concurrence vanishes at the opening angle $\theta = \pi/2$. This behavior is well understood from Eqs. (11) and (14) as well as from the conservation of the projection $M_{\rm tot}$ of the total angular momentum $J_{\rm tot}$ of the overall system of an ion plus two photons. Namely, if no electron-spin flip were to occur during the $2s_{1/2} \to 1s_{1/2}$ decay and assuming zero nuclear spin, the conservation law enforces that the change of the projection of the ion's total angular momentum relative to the quantization axis z (chosen along the momentum of the first photon) would be given by $M_i - M_f = 0 = \lambda_1 + M_{\gamma_2}$. In this expression, λ_1 is the helicity of the first photon and M_{γ_2} is the projection of the angular momentum of the second photon. For photons emitted in parallel or back to back, this projection is $M_{\gamma_2} = \lambda_2$ and $-\lambda_2$, correspondingly, thus leading to the conditions $\lambda_1 = -\lambda_2$ or $\lambda_1 = \lambda_2$. Moreover, owing to the spherical symmetry of s-ionic states there is an equal probability of emission of the first photon with helicity $\lambda_1 = +1$ or -1. This immediately implies maximally entangled Bell states $|\Psi\rangle = (|+-\rangle + |+-\rangle)/\sqrt{2}$ for $\theta = 0$ and $|\Psi\rangle = (|++\rangle + |--\rangle)/\sqrt{2}$ for $\theta = \pi$, as predicted by Eqs. (11) and (12).

Similar to the cases of parallel and back-to-back photon emission, the conservation condition $\lambda_1 = -M_{\gamma_2}$ with the helicity of the first photon being $\lambda_1 = \pm 1$ may help explain the behavior of the entanglement measure $C(\theta)$ at $\theta = \pi/2$. This will require us to return to Eq. (9), which simplifies—within the dipole approximation—to

$$\vec{\mathcal{A}}_\lambda = -\sqrt{6\pi}\sum_{M_\gamma=-1}^{1} \lambda\,\hat{a}^{p=1}_{1M_\gamma}(k)\,d^1_{M_\gamma\lambda}(\theta), \quad (24)$$

where $d^1_{M_\gamma\lambda}(\theta)$ is Wigner's (small) d matrix, whose properties are discussed in detail in Ref. [28]. For the opening angle

$\theta = \pi/2$, the elements of this matrix are $d^1_{11} = d^1_{1-1} = d^1_{-11} = d^1_{-1-1} = 1/2$, implying, together with Eq. (6) and the fact that the ionic states are spherically symmetric, that the probability for the second photon to have projection $M_{\gamma_2} = \mp 1$ on the quantization axis of the overall system is independent of its helicity λ_2. Therefore, no correlations between the polarization (spin) states of the emitted photons appear for the perpendicular emission, thus leading to the vanishing entanglement $C(\pi/2) = 0$, as displayed in Fig. 2.

2. *Purity of the two-photon state and impact on entanglement*

As seen from the top panel of Fig. 2, the accuracy of the nonrelativistic approximation [Eq. (23)] becomes generally worse if one of the photons has a significantly higher energy than the other one. For the $2s_{1/2} \to 1s_{1/2}$ transition of hydrogenlike uranium, for example, the nonrelativistic dipole approximation overestimates the concurrence measure by about 10% for forward as well as backward opening angles, for an energy sharing $\eta = 1/16$. In order to understand better such an energy-dependent behavior, we study the purity of the two-photon polarization state, defined as

$$\mathcal{P} = \tfrac{4}{3}\,\mathrm{Tr}(\hat{\rho}_\gamma^2) - \tfrac{1}{3}, \tag{25}$$

where $\hat{\rho}_\gamma$ represents the photon density matrix [Eq. (10)]. The purity varies from $\mathcal{P} = 0$ (completely mixed state) to $\mathcal{P} = 1$ (pure state). In Fig. 3 we display the purity $\mathcal{P}$ for the $2s_{1/2} \to 1s_{1/2}$ decay of U^{91+} for two relative photon energies: $\eta = 1/16$ (upper panel) and $\eta = 1/2$ (lower panel). As seen from the figure, the purity strongly depends on the energy-sharing parameter: While the purity of the two-photon state is always greater than 0.987 for an equal energy sharing $\eta = 0.5$, it is significantly reduced for $\eta = 1/16$. The loss of purity can be attributed to the spin-orbit coupling in hydrogenlike ions as well as to the magnetic terms in the electron-photon interaction. Both of these relativistic effects increase with the nuclear charge Z and with the photon energy ω. They lead to the fact that the decay of the unpolarized and hence mixed $2s_{1/2}$ level results in the emission of photons characterized by a partially mixed state. Due to complementarity of entanglement, mixedness and purity of a quantum mechanical state [33], such a loss of purity causes the reduction of the concurrence measure, which can be observed in the top panel of Fig. 2. Despite such a reduction, there are still quantum correlations between the polarization states of the photons.

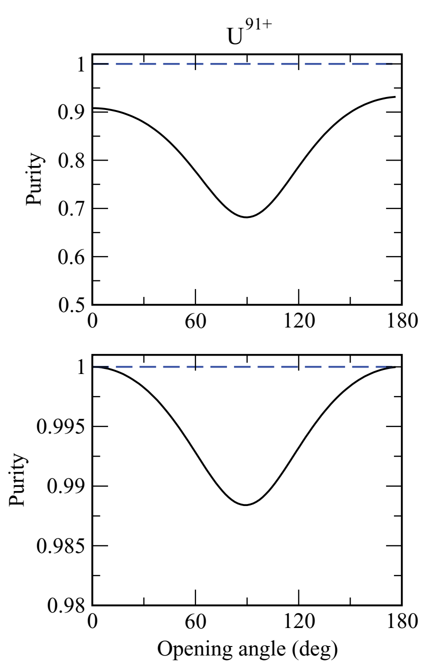

FIG. 3. (Color online) Purity [Eq. (25)] of the two-photon state in the $2s_{1/2} \to 1s_{1/2}$ decay of hydrogenlike uranium. Results of the nonrelativistic dipole approximation (dashed line) and a rigorous relativistic treatment (solid line) are shown for relative photon energies $\eta = 1/16$ (upper panel) and $\eta = 1/2$ (lower panel).

B. Heliumlike ions

1. $1s_{1/2}\,2s_{1/2}\,{}^1S_0 \to 1s^2_{1/2}\,{}^1S_0$ *transition*

In contrast to the $2s_{1/2} \to 1s_{1/2}$ decay of one-electron systems, the $1s_{1/2}\,2s_{1/2}\,{}^1S_0 \to 1s^2_{1/2}\,{}^1S_0$ transition in heliumlike ions always proceeds between the pure $J = 0$ quantum-mechanical states [see Eq. (1)]. Therefore, the spin state of the photon pair emitted in such a transition will be pure at any energy sharing. The concurrence measure $C(\theta)$ of such a pure state calculated within the exact relativistic theory turns out to be almost identical to the dipole approximation [Eq. (23)]. The deviation between both predictions does not exceed 1%, even for the heaviest heliumlike ions, and arises due to the higher, nondipole terms in the electron-photon interaction [Eq. (8)]. By comparing this prediction with the calculations performed in Sec. V A for hydrogenlike ions, we again argue that the reduction of the spin entanglement between the photons emitted in the $2s_{1/2} \to 1s_{1/2}$ transition shall be mainly attributed to the loss of purity of ionic states.

2. $1s_{1/2}\,2p_{1/2}\,{}^3P_0 \to 1s^2_{1/2}\,{}^1S_0$ *transition*

After the preceding, brief discussion of the $1s_{1/2}\,2s_{1/2}\,{}^1S_0 \to 1s^2_{1/2}\,{}^1S_0$ transition, we turn now to explore quantum correlations in the $1s_{1/2}\,2p_{1/2}\,{}^3P_0 \to 1s^2_{1/2}\,{}^1S_0$ decay. As one can expect from the spin-state vector [Eq. (17)] derived in the leading order, electric and magnetic dipole approximation, these correlations should differ from those predicted for the $S \to S$ cases. Indeed, by inserting the vector [Eq. (17)] into Eq. (23), we obtain—within the dipole ($E1M1$) approximation—the concurrence measure as

$$\mathcal{C}(\theta,\eta) = \left| \frac{\Delta^2(\eta)\cos^4\frac{\theta}{2} - \Sigma^2(\eta)\sin^4\frac{\theta}{2}}{\Delta^2(\eta)\cos^4\frac{\theta}{2} + \Sigma^2(\eta)\sin^4\frac{\theta}{2}} \right|. \tag{26}$$

In contrast to the polarization entanglement [Eq. (23)] between the photons emitted in the $S \to S$ transitions, here the concurrence turns out to depend on the photons' energy sharing. To better understand such a dependence, we display the entanglement of the photons emitted in the $1s_{1/2}\,2p_{1/2}\,{}^3P_0 \to 1s^2_{1/2}\,{}^1S_0$ decay of heliumlike xenon and uranium ions in Fig. 4. Calculations are performed for two relative energies $\eta = 1/10$ and $1/4$, both within the dipole approximation [Eq. (26)], and by using the exact theory, which accounts for the higher-multipole channels. As seen from the figure, both theoretical approximations predict maximal entanglement

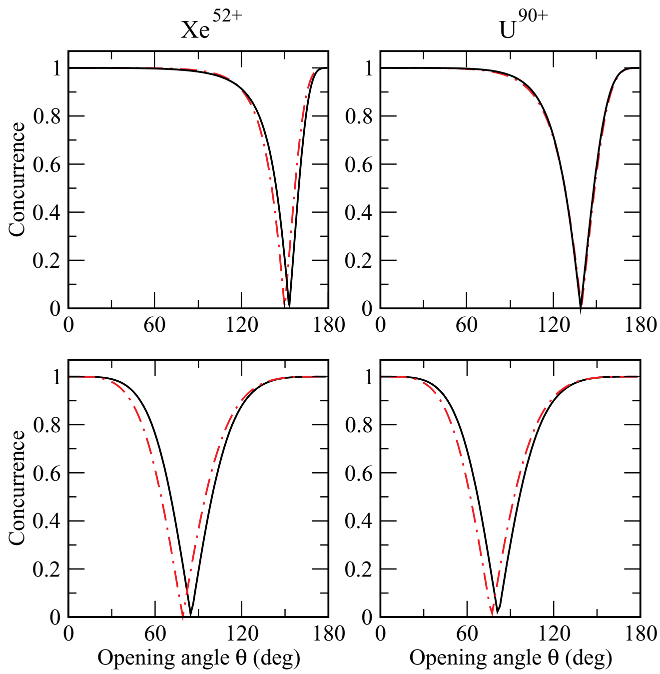

FIG. 4. (Color online) Concurrence of two photons emitted in the $1s_{1/2}\,2p_{1/2}\,{}^3P_0 \to 1s_{1/2}^2\,{}^1S_0$ decay of heliumlike xenon and uranium ions. Results of the $E1M1$ dipole approximation (dash-dotted line) and of the rigorous relativistic theory (solid line) are shown for two relative photon energies $\eta = 1/10$ (upper panel) and $\eta = 1/4$ (lower panel).

$\mathcal{C} = 1$ for the parallel and back-to-back photon emission at any energy sharing η, a feature that could be expected from the conservation laws. In contrast, the critical opening angle θ_c at which the concurrence vanishes, $\mathcal{C}(\theta_c) = 0$, varies with the relative photon energy. By inspecting Eq. (26) we find the following relation for this angle:

$$\tan^2\left(\frac{\theta_c}{2}\right) = \frac{|\Delta(\eta)|}{|\Sigma(\eta)|}. \qquad (27)$$

It follows from this expression that for any nonzero values of the functions $\Delta(\eta)$ and $\Sigma(\eta)$ there exists one single critical angle $\theta_c(\eta)$, as can also be seen, for example, from Fig. 4.

If the photons emitted in the $1s_{1/2}\,2p_{1/2}\,{}^3P_0 \to 1s_{1/2}^2\,{}^1S_0$ decay carry away the same portion of energy $\omega_1 = \omega_2$, the function $\Delta(\eta)$ turns out to be zero and Eq. (27) cannot be applied for the determination of the critical angle θ_c. As can be seen from Eqs. (18) and (26), in this case the photons' state is maximally entangled (a Bell state) for any opening angle, i.e., $\mathcal{C}(\theta,0.5) = 1$. This behavior differs from that of the $1s_{1/2}\,2s_{1/2}\,{}^1S_0 \to 1s_{1/2}^2\,{}^1S_0$ and $2s_{1/2} \to 1s_{1/2}$ transitions for which no correlations appear at the opening angle $\theta = \pi/2$. In order to understand the reason for this difference we shall return to Eqs. (6)–(9). By making use of these expressions and the properties of the Wigner matrices we rewrite the two-photon transition amplitude in terms of reduced matrix elements as

$$\mathcal{M}_{fi}^{\vec{k}_1\vec{k}_2}(\lambda_1,\lambda_2) \propto (\lambda_1 + \lambda_2)[S_{E1M1}(\omega) + S_{M1E1}(\omega)], \qquad (28)$$

where, for the case of equal energy sharing, $\omega_1 = \omega_2 = \omega$. It follows from Eq. (28) that, apart from the conservation of the projection of the total angular momentum $J_{\rm tot}$ discussed in Sec. V A, an additional selection rule arises for the $1s_{1/2}\,2p_{1/2}\,{}^3P_0 \to 1s_{1/2}^2\,{}^1S_0$ transition that forbids emission of the photons with opposite helicities. Together with the equal probabilities of the spin states $|{++}\rangle$ and $|{--}\rangle$, this selection rule implies the Bell state [Eq. (18)] and hence maximal engagement of the photons' state.

3. *Incoherent preparation of the ions:* $1s_{1/2}\,2s_{1/2}\,{}^3S_1 \to 1s_{1/2}^2\,{}^1S_0$ *transition*

Until now our discussion of the two-photon decay of heliumlike ions was restricted to $J = 0 \to J = 0$ transitions. In this case, both initial and final ionic states are pure along the entire isoelectronic sequence and, consequently, the two-photon states are pure as well. In order to underline again the effect of the loss of purity on the quantum correlations, we study the two-photon decay of the unpolarized $1s_{1/2}\,2s_{1/2}\,{}^3S_1$ state. In Fig. 5 we display the degree of spin entanglement for the $1s_{1/2}\,2s_{1/2}\,{}^3S_1 \to 1s_{1/2}^2\,{}^1S_0$ transition in heliumlike xenon and uranium ions. Again, the exact relativistic calculations are compared with the predictions of the electric dipole ($E1E1$) approach for two relative energies $\eta = 1/10$ and $1/4$. As seen from the figure, the general behavior of the measure $\mathcal{C}_{{}^3S_0 \to {}^1S_0}$ is similar to that of the $1s_{1/2}\,2s_{1/2}\,{}^1S_0 \to 1s_{1/2}^2\,{}^1S_0$ and $2s_{1/2} \to 1s_{1/2}$ transitions. Namely, the concurrence changes from $\mathcal{C}_{{}^3S_0 \to {}^1S_0} = 1$ for the parallel photon emission down to zero at $\theta = \pi/2$ and back to a maximum entanglement for $\theta = \pi$. Similar to the discussion in Sec. V A, this can be easily understood if one applies again the momentum projection selection rules and Eq. (24). In contrast to the $1s_{1/2}\,2s_{1/2}\,{}^1S_0 \to$

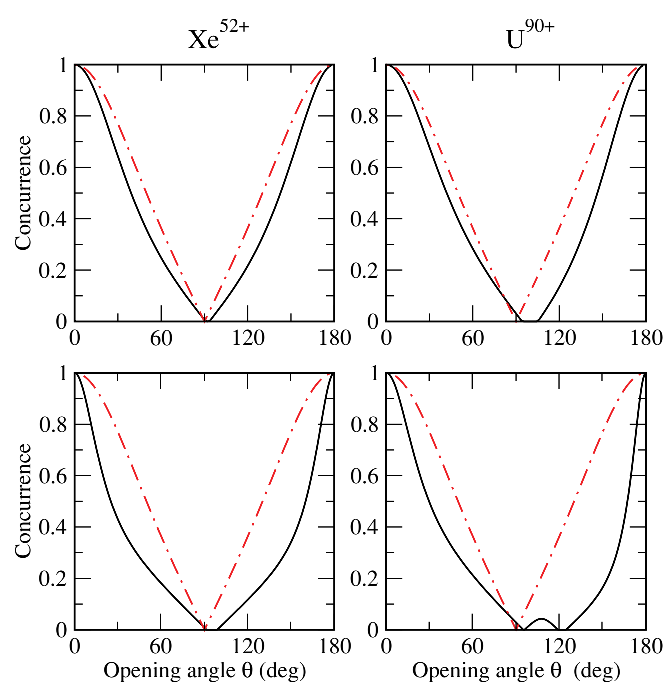

FIG. 5. (Color online) Concurrence of two photons emitted in the $1s_{1/2}\,2s_{1/2}\,{}^3S_1 \to 1s_{1/2}^2\,{}^1S_0$ decay of heliumlike xenon and uranium ions. Results of the $E1E1$ dipole approximation (dash-dotted line) and the rigorous relativistic theory (solid line) are shown for two relative photon energies $\eta = 1/10$ (upper panel) and $\eta = 1/4$ (lower panel).

$1s_{1/2}^2\,{}^1S_0$ and $2s_{1/2} \to 1s_{1/2}$ transitions, however, the degree of entanglement $\mathcal{C}_{^3S_0 \to ^1S_0}$ decreases much faster for the forward $0 < \theta < \pi/3$ and backward $2\pi/3 < \theta < \pi$ angles, an effect that can be understood if we remember that the initial ionic state is prepared in an unpolarized (mixed) state.

As one can see from Fig. 5, spin entanglement for the $1s_{1/2}\,2s_{1/2}\,{}^3S_1 \to 1s_{1/2}^2\,{}^1S_0$ transition is very sensitive to higher multipoles in the electron-photon interaction. This is a direct consequence of a strong suppression of the $E1E1$ decay channel caused by the symmetry properties of the multiphoton systems as described by Bose statistics (see Refs. [34–40] for further details). The nondipole contributions become more significant for heavier ions and with increasing energy sharing η $(0 < \eta < 0.5)$ and result in an asymmetric shift in the concurrence.

VI. CONCLUSION

In summary, the two-photon decay of few-electron ions has been investigated within the framework of density-matrix and second-order perturbation theory. In our study special attention has been paid to the quantum correlations between the spin states of the emitted photons. By making use of the nonrelativistic dipole model, we derived a simple analytical expression for such spin entanglement if observed in $2s_{1/2} \to 1s_{1/2}$ and $1s_{1/2}\,2s_{1/2}\,{}^1S_0 \to 1s_{1/2}^2\,{}^1S_0$ transitions in hydrogen and heliumlike ions, respectively. By comparing the predictions of the dipole approximation with the fully relativistic calculations, we were able to explore the influence of the relativistic effects on the photon polarization properties. In particular, we observed a reduction of entanglement that becomes greater for high-Z systems and can be attributed to the loss of purity of the two-photon spin states induced by higher-multipole contributions and the relativistic contraction of the wave functions.

In addition to the well-established $2s_{1/2} \to 1s_{1/2}$ and $1s_{1/2}\,2s_{1/2}\,{}^1S_0 \to 1s_{1/2}^2\,{}^1S_0$ transitions, entanglement studies were also performed for the $1s_{1/2}\,2s_{1/2}\,{}^3S_1 \to 1s_{1/2}^2\,{}^1S_0$ and $1s_{1/2}\,2p_{1/2}\,{}^3P_0 \to 1s_{1/2}^2\,{}^1S_0$ decays of intermediate- and high-Z heliumlike ions. Based on the independent-particle model, which is a good approximation for the analysis of the bound-bound transitions in heavy atomic systems, we found that the concurrence is very sensitive to the relative energy of emitted photons, as well as to the higher-multipole contributions to the electron-photon interaction. The strongest nondipole effects have been identified for the $1s_{1/2}\,2s_{1/2}\,{}^3S_1 \to 1s_{1/2}^2\,{}^1S_0$ two-photon transition for which the $E1E1$ decay channel is forbidden due to symmetry properties of the system.

Our theoretical analysis, performed for the intermediate- and high-Z domain, underlines the importance of a detailed knowledge of the electronic structure of ions (atoms) for a better understanding of two-photon entanglement. This is rather different from the earlier studies on the decay of light neutral atoms [16–18] where the quantum correlations between the photons could be predicted solely from angular momentum conservation. In contrast, for heavy ions, entanglement properties of the photon pairs are governed by the complicated interplay between these conservation laws and relativistic as well as many-body effects.

The spin quantum correlation studies reported in the present work may help explain the outcome of future γ-γ coincidence measurements. Apart from the analysis of relativistic and quantum electrodynamics effects, parity-violation corrections to the photon spin entanglement can be observed in such coincidence experiments. A theoretical analysis of these parity-violation phenomena is currently under way.

ACKNOWLEDGMENTS

The authors would like to thank the organizers of the workshop Energiereiche Atomare Stösse meeting in Riezlern where this work was initiated. A.S. and F.F. acknowledge support from the Helmholtz Gemeinschaft under Project No. VH-NG-421. M.C.T. acknowledges financial support by Studienstiftung des Deutschen Volkes and by Deutsche Forschungsgemeinscchaft Research Unit FG760.

[1] M. Göppert-Mayer, Ann. Phys. (Leipzig) **9**, 273 (1931).
[2] G. Breit and E. Teller, Astrophys. J. **91**, 215 (1940).
[3] S. Klarsfeld, Phys. Lett. A **30**, 382 (1969).
[4] C. K. Au, Phys. Rev. A **14**, 531 (1976).
[5] J. H. Tung, X. M. Ye, G. J. Salamo, and F. T. Chan, Phys. Rev. A **30**, 1175 (1984).
[6] S. P. Goldman and G. W. F. Drake, Phys. Rev. A **24**, 183 (1981).
[7] X. M. Tong, J. M. Li, L. Kissel, and R. H. Pratt, Phys. Rev. A **42**, 1442 (1990).
[8] J. P. Santos, F. Parente, and P. Indelicato, Eur. Phys. J. D **3**, 43 (1998).
[9] A. Surzhykov, P. Koval, and S. Fritzsche, Phys. Rev. A **71**, 022509 (2005).
[10] U. D. Jentschura and A. Surzhykov, Phys. Rev. A **77**, 042507 (2008).
[11] R. Marrus and R. W. Schmieder, Phys. Rev. A **5**, 1160 (1972).
[12] P. H. Mokler and R. W. Dunford, Phys. Scr. **69**, C1 (2004).
[13] K. Ilakovac, M. Uroić, M. Majer, S. Pasić, and B. Vuković, Radiat. Phys. Chem. **75**, 1451 (2006).
[14] A. Kumar *et al.*, Eur. Phys. J. Spec. Top. **169**, 19 (2009).
[15] S. Trotsenko *et al.*, Phys. Rev. Lett. **104**, 033001 (2010).
[16] A. Aspect, J. Dalibard, and G. Roger, Phys. Rev. Lett. **49**, 1804 (1982).
[17] W. Perrie, A. J. Duncan, H. J. Beyer, and H. Kleinpoppen, Phys. Rev. Lett. **54**, 1790 (1985).
[18] H. Kleinpoppen, A. J. Duncan, H.-J. Beyer, and Z. A. Sheikh, Phys. Scr. T **72**, 7 (1997).
[19] A. Einstein, B. Podolsky, and N. Rosen, Phys. Rev. **47**, 777 (1935).
[20] P. A. Schilpp, *Albert Einstein: Philosopher-Scientist* (Open Court, Chicago, 1949), pp. 224–228.
[21] T. Radtke, A. Surzhykov, and S. Fritzsche, Eur. Phys. J. D **49**, 7 (2008).

[22] T. Radtke, A. Surzhykov, and S. Fritzsche, Phys. Rev. A **77**, 022507 (2008).
[23] A. Surzhykov, U. D. Jentschura, Th. Stöhlker, and S. Fritzsche, Eur. Phys. J. D **46**, 27 (2008).
[24] A. Surzhykov, A. Volotka, F. Fratini, J. P. Santos, P. Indelicato, G. Plunien, Th. Stöhlker, and S. Fritzsche, Phys. Rev. A **81**, 042510 (2010).
[25] M. C. Tichy, F. de Melo, M. Kuś, F. Mintert, and A. Buchleitner, e-print arXiv:0902.1684.
[26] P. Lambropoulos, C. Kikuchi, and R. K. Osborn, Phys. Rev. **144**, 1081 (1966).
[27] S. Carusotto, G. Fornaca, and E. Polacco, Phys. Rev. **157**, 1207 (1967).
[28] V. V. Balashov, A. N. Grum-Grzhimailo, and N. M. Kabachnik, *Polarization and Correlation Phenomena in Atomic Collisions* (Springer-Verlag, Berlin, 2000).
[29] G. W. F. Drake and S. P. Goldman, Phys. Rev. A **23**, 2093 (1981).
[30] A. Maquet, V. Véniard, and T. A. Marian, J. Phys. B **31**, 3743 (1998).
[31] M. E. Rose, *Elementary Theory of Angular Momentum* (Wiley, New York, 1963).
[32] W. K. Wootters, Phys. Rev. Lett. **80**, 2245 (1998).
[33] M. Jakob and J. A. Bergou, e-print arXiv:quant-ph/0302075.
[34] R. W. Dunford, Phys. Rev. A **69**, 062502 (2004).
[35] D. DeMille, D. Budker, N. Derr, and E. Deveney, Phys. Rev. Lett. **83**, 3978 (1999).
[36] L. D. Landau, Dokl. Akad. Nauk SSSR **60**, 207 (1948).
[37] C. N. Yang, Phys. Rev. **77**, 242 (1950).
[38] J. Shapiro and G. Breit, Phys. Rev. **113**, 179 (1959).
[39] D. O'Connell, K. J. Kollath, A. J. Duncan, and H. Kleinpoeppen, J. Phys. B **8**, L214 (1975).
[40] H. Krüger and A. Oed, Phys. Lett. A **54**, 251 (1975).